



# Native lysozyme and dry-heated lysozyme interactions with membrane lipid monolayers: Lateral reorganization of LPS monolayer, model of the *Escherichia coli* outer membrane

Melanie Derde<sup>a,b,\*</sup>, Françoise Nau<sup>a,b</sup>, Valérie Lechevalier<sup>a,b</sup>, Catherine Guérin-Dubiard<sup>a,b</sup>, Gilles Paboeuf<sup>c</sup>, Sophie Jan<sup>a,b</sup>, Florence Baron<sup>a,b</sup>, Michel Gautier<sup>a,b</sup>, Véronique Vié<sup>c,\*\*</sup>

<sup>a</sup> Agrocampus Ouest, UMR1253 Science et Technologie du Lait et de l'Oeuf, F-35042 Rennes, France

<sup>b</sup> INRA, UMR1253 Science et Technologie du Lait et de l'Oeuf, F-35042 Rennes, France

<sup>c</sup> Université de Rennes 1, Institut de Physique de Rennes, UMR6251, CNRS, F-35042 Rennes, France

## ARTICLE INFO

### Article history:

Received 22 May 2014

Received in revised form 26 September 2014

Accepted 20 October 2014

Available online 27 October 2014

### Keywords:

BAM

AFM

Langmuir film

Dry-heated lysozyme

LPS monolayer

## ABSTRACT

Lysozyme is mainly described active against Gram-positive bacteria, but is also efficient against some Gram-negative species. Especially, it was recently demonstrated that lysozyme disrupts *Escherichia coli* membranes. Moreover, dry-heating changes the physicochemical properties of the protein and increases the membrane activity of lysozyme. In order to elucidate the mode of insertion of lysozyme into the bacterial membrane, the interaction between lysozyme and a LPS monolayer mimicking the *E. coli* outer membrane has been investigated by tensiometry, ellipsometry, Brewster angle microscopy and atomic force microscopy. It was thus established that lysozyme has a high affinity for the LPS monolayer, and is able to insert into the latter as long as polysaccharide moieties are present, causing reorganization of the LPS monolayer. Dry-heating increases the lysozyme affinity for the LPS monolayer and its insertion capacity; the resulting reorganization of the LPS monolayer is different and more drastic than with the native protein.

© 2014 Elsevier B.V. All rights reserved.

## 1. Introduction

Antibiotic resistance due to decades of misuse in human and veterinary medicine is causing an enormous public health problem. Several pathogens, such as *Staphylococcus aureus* and *Klebsiella pneumoniae*, have developed multiple antibiotic resistance mechanisms. The consequence is difficult and expensive treatments of several diseases [1]. The number of these multi-resistant strains is increasing, but only three new antibiotic molecules against Gram-positive multiresistant strains were registered since 1970, and none for Gram-negative multiresistant strains [2]. Research for novel antimicrobial compounds is thus needed, besides the measures of the European Union to limit the spread of antibiotic resistances. Preferably, novel compounds should decrease the development rate and spread of antibiotic resistance.

Several natural proteins and peptides can be considered as potential candidates, especially the antimicrobial proteins or peptides (AMP) which act on the bacterial membranes. Their target, i.e. the bacterial cell membrane, is a generalized and vital target, and thus antimicrobial resistance development remains limited [3,4]. AMPs are mostly positively charged molecules, amphiphilic, flexible, and contain several hydrophobic residues, suggesting electrostatic and hydrophobic interactions with the bacterial cell membrane [3]. These interactions can then lead to the membrane disruption, causing bacterial cell death or translocation of the AMP into the cytoplasm where these can interact with several intracellular targets [3,5].

One of the natural antimicrobial proteins, widely studied, is hen egg white lysozyme. This small enzyme (129 amino acid residues) was for a long time only known for its antimicrobial activity against Gram-positive bacteria, due to its muramidase activity [6,7]. However, several studies suggest other mechanisms of action against both Gram-positive and Gram-negative bacteria, such as perturbation of DNA or RNA synthesis, activation of autolysin production, and membrane permeabilization [7–10]. The disruption of both the outer and cytoplasmic membranes of *Escherichia coli* by native lysozyme has been recently demonstrated in our laboratory [9]. Especially, pore formation in the outer membrane of *E. coli* has been described [11]. Moreover, pore size and/or quantity were higher with dry-heated lysozyme as compared to the native protein [11]. The physicochemical modifications

**Abbreviations:** AFM, Atomic force microscopy; AMP, Antimicrobial peptide or protein; BAM, Brewster angle microscopy; DH-L, Dry-heated lysozyme; HEPES, 4-(2-Hydroxyethyl) piperazine-1-ethanesulfonic acid; KLA, Lipid A-(KdO)<sub>2</sub>; LPS, Lipopolysaccharides; MIP, Maximum insertion pressure; N-L, Native lysozyme

\* Correspondence to: M. Derde, Agrocampus Ouest, INRA, UMR 1253 STLO, 65, rue de St-Brieuc, 35042 Rennes, France. Tel.: +33 2 23 48 55 74.

\*\* Correspondence to: V. Vié, Université de Rennes 1, Institut de Physique de Rennes (IPR), 263, Av Général Leclerc, F-35042 Rennes Cedex. Tel.: +33 2 23 23 56 45.

E-mail addresses: [melanie.derde@agrocampus-ouest.fr](mailto:melanie.derde@agrocampus-ouest.fr) (M. Derde), [veronique.vie@univ-rennes1.fr](mailto:veronique.vie@univ-rennes1.fr) (V. Vié).

resulting from dry-heating are an increased positive charge at physiological pH as well as increased flexibility and hydrophobicity while preserving the secondary and tertiary structure; these modifications could be responsible for the enhanced antibacterial activity of dry-heated lysozyme, similarly to what has been described for lysozyme modification by enzyme hydrolysis, heat denaturation, or fusion with several chemical moieties [7,12–17].

However, the interactions between the outer membrane lipids of Gram-negative bacteria and both types of lysozyme (native and dry-heated) remain to be investigated. In the presently reported study, lipopolysaccharide (LPS) monolayers of *E. coli* K12 have been used as a model for the bacterial outer membrane [18,19]. These LPS monolayers were formed in a Langmuir trough at a controlled initial surface pressure ( $\pi_{\text{initial}}$ ). Multiscale analysis of the interfacial film using tensiometry, ellipsometry, Brewster angle microscopy (BAM) and atomic force microscopy (AFM), enabled to investigate the LPS–lysozyme interactions, to study the consequences of lysozyme interaction on the LPS monolayer.

## 2. Materials and methods

### 2.1. Proteins and lipids

Native lysozyme (N-L) powder (pH 3.2) was obtained from Liot (Annezin, 62-France). It was heated for 7 days at 80 °C in hermetically closed glass tubes to obtain dry-heated lysozyme (DH-L). Lysozyme (N-L or DH-L) was solubilized (around 0.5 g/L) in 5 mM 4-(2-hydroxyethyl)piperazine-1-ethanesulfonic acid (HEPES) buffer (Sigma Aldrich, Saint-Quentin, France), pH 7.0, 150 mM NaCl (Fluka, Saint-Quentin, France). The concentration of the lysozyme stock solution was precisely determined by absorbance at 280 nm (extinction coefficient = 2.6 L/(g·cm)) [20]. The protein solution was then diluted in the HEPES buffer to obtain the desired concentration for used lysozyme solutions.

The lipopolysaccharides (LPS) of *E. coli* K12 were obtained from Invivogen (Toulouse, France). The LPS were solubilized in 2:1 chloroform/methanol mixture at 0.5 g/L. Lipid A-(KdO)<sub>2</sub> (KLA) were purchased by Avanti Polar Lipids (Alabaster, Alabama, USA) and were solubilized in a 2:1 chloroform/methanol mixture at 0.67 g/L.

### 2.2. Lipid/protein monolayers

The experiments were performed in a homemade TEFLON® trough of 8 ml at 20 °C. Before each use, the trough was thoroughly cleaned with successively warm tap water, ethanol, demineralized water, and then boiled for 15 min in demineralized water. After cooling the TEFLON® trough was then filled with 8 ml HEPES buffer. The LPS or KLA were spread with a high precision Hamilton microsyringe at the clean air/liquid interface to obtain an initial surface pressure between 18 and 30 mN/m. After 1 h to allow the solvent to evaporate and the lipids to organize, 50  $\mu$ l N-L or DH-L solution were injected in the subphase with a Hamilton syringe to obtain a final protein concentration of 0.02, 0.03, 0.05, 0.1, 0.2, 0.3 or 1  $\mu$ M.

### 2.3. Surface pressure measurements

The surface pressure was measured following a Wilhelmy method using a 10 mm  $\times$  22 mm filter paper as plate (Whatman, Velizy-Villacoublay, France) connected to a microelectronic feedback system (Nima PS4, Manchester, England). The surface pressure ( $\pi$ ) was recorded every 4 s with a precision of  $\pm 0.2$  mN/m. The measured surface pressure is the result of the surface tension of water minus the surface tension of the lipid film.

### 2.4. Ellipsometry

Measurements of the ellipsometric angle value were carried out with an in-house automated ellipsometer in a “null ellipsometer” configuration [21,22]. A polarized He–Ne laser beam ( $\lambda = 632.8$  nm, Melles Griot, Glan-Thompson polarizer) was reflected on the surface of the trough. The incidence angle was 52.12°, i.e. Brewster angle for the air/water interface minus 1°. After reflection on the liquid surface, the laser light passed through a  $\lambda/4$  retardation plate, a Glan-Thompson analyzer, and a photomultiplier. The analyzer angle, multiplied by two, yielded the value of the ellipsometric angle ( $\Delta$ ), i.e. the phase difference between parallel and perpendicular polarization of the reflected light. The laser beam probed the 1 mm<sup>2</sup> surface with a depth in the order of 1  $\mu$ m. Initial values of the ellipsometric angle ( $\Delta_0$ ) and surface pressure of buffer solutions were recorded for at least half an hour to assure that the interface is clean. Only in the case of a stable, minimal signal, experiments were performed. Values of  $\Delta$  were recorded every 4 s with a precision of  $\pm 0.5^\circ$ . When measuring the pressure increase induced by lysozyme at the air/liquid interface, a lysozyme solution at 0.1  $\mu$ M is deposited in the trough. When the pressure increase induced by lysozyme is measured at the LPS/liquid interface, a LPS monolayer is first created as formerly described.

For the detection of local ellipsometric angle values, an imaging ellipsometer EP3 (Nanofilm, Göttingen, Germany) in “null ellipsometer” configuration was used with a 10 $\times$  objective. A solid-state laser ( $\lambda = 532$  nm) was used as a light source. Delta/psi maps were recorded with the EP3 software for a 450  $\mu$ m  $\times$  390  $\mu$ m surface. For delta and psi maps, a polarizer and analyzer range of 20° was used. Delta/psi maps were based on 20 images taken at different polarizer and analyzer angles.

### 2.5. Brewster angle microscopy

An ellipsometer EP3 (Nanofilm, Berlin, Germany) with a polarized incident laser ( $\lambda = 532$  nm) was used with a 10 $\times$  objective in a Brewster angle configuration (angle of incidence was 53.1°). The images represented a 450  $\mu$ m  $\times$  390  $\mu$ m surface. Different zones of each sample were evaluated; the images here shown are representative of the whole samples.

### 2.6. AFM sample preparation and AFM imaging

Experiments were performed with a computer-controlled and user-programmable Langmuir TEFLON®-coated trough (type 601BAM) equipped with two movable barriers and of total surface 90 cm<sup>2</sup> (Nima Technology Ltd., England). Before starting the experiments, the trough was cleaned successively with ultrapure water (Nanopure-UV), ethanol, and finally ultrapure water. The trough was filled with 5 mM HEPES buffer pH 7 150 mM NaCl. LPS were spread over the clean air/liquid interface at a surface pressure of 25 mN/m or 30 mN/m. The solvent was then left to evaporate for 1 h. Then, a Langmuir–Blodgett transfer was performed onto freshly cleaved mica plates at constant surface pressure by vertically raising (1 mm/min) the mica through the air/liquid interface to obtain a sample of the initial LPS monolayer. The LPS monolayer stability was assured during the Langmuir–Blodgett transfer allowing the injection of lysozyme in the subphase.

Then, 0.1  $\mu$ M lysozyme was injected in the subphase of the previously sampled LPS monolayer with a Hamilton syringe. Surface pressure variations were recorded until a stable surface pressure was reached (after  $\sim 1$  h). Then, a second Langmuir–Blodgett transfer was performed onto freshly cleaved mica as described above to obtain the sample of the LPS monolayer after lysozyme interaction.

AFM imaging of Langmuir–Blodgett films was performed in contact mode using a Pico-plus atomic force microscope (Agilent Technologies, Phoenix, AZ) under ambient conditions with a scanning area of 20  $\times$  20  $\mu$ m<sup>2</sup> and 5  $\times$  5  $\mu$ m<sup>2</sup>. Topographic images were acquired using

silicon nitride tips on integral cantilevers. The forces were controlled along the imaging process. Different zones of each sample were scanned; the images here shown are representative of the whole samples.

### 3. Results

#### 3.1. Insertion capacity of lysozyme into a LPS monolayer

The insertion capacity of N-L and DH-L into a LPS monolayer was determined by independent tensiometry experiments at different protein concentrations. Insertion can be detected by a surface pressure increase ( $\Delta\pi = \pi_{\text{final}} - \pi_{\text{initial}}$ ). Here, lysozyme was injected under a LPS monolayer with an initial surface pressure ( $\pi_{\text{initial}}$ ) of 18 mN/m.

In both cases (N-L and DH-L), a surface pressure increase is demonstrated indicating lysozyme insertion into the LPS monolayer for protein concentrations above 0.02  $\mu\text{M}$  (Fig. 1A). Below 0.05  $\mu\text{M}$ , no difference can be observed between both lysozymes, while above this protein concentration, DH-L induces a higher surface pressure increase than N-L (Fig. 1A). When increasing the lysozyme subphase concentration, a  $\Delta\pi$ -plateau is obtained at a lysozyme concentration of 0.2  $\mu\text{M}$  for both N-L and DH-L, indicating saturation of the interface in these conditions. However, the maximum  $\Delta\pi$  value is higher for DH-L than for N-L (12 mN/m and 8 mN/m, respectively; Fig. 1A). For further investigation of the insertion capacity of lysozyme, 0.1  $\mu\text{M}$  N-L or DH-L has been used. At this concentration, differences exist between both proteins, and lipid protein interactions can be observed, while minimizing protein-protein interactions in the bulk solution (aggregation) or at the lipid interface.

#### 3.2. Affinity of lysozyme for LPS monolayers

To evaluate the affinity of both N-L and DH-L for the LPS monolayer,  $\Delta\pi$  was determined after lysozyme injection (0.1  $\mu\text{M}$ ) under LPS monolayers previously formed at different initial surface pressures ( $\pi_{\text{initial}}$ ). Supplementary experiments demonstrated that no phase transition occurs in the  $\pi$ -range here used (supplementary data S3); comparisons are then valuable. Linear regression analysis of the  $\Delta\pi$  values versus  $\pi_{\text{initial}}$  allows calculation of three binding parameters of lysozyme: maximal insertion pressure (MIP), synergy factor, and  $\Delta\pi_0$  (Fig. 1B) [23–25]. MIP is the intercept of the straight line with x-axis after extrapolation; it is thus the initial surface pressure for which no surface pressure increase occurs when lysozyme is injected in the subphase. The synergy factor is determined as the slope of the linear regression + 1. The synergy factor provides information on the affinity of the protein for the lipid monolayer. High positive synergy values indicate the existence of strong protein/lipid interactions, since it means that the protein is able to insert into the lipid film even when initial surface pressure is high.  $\Delta\pi_0$  is the

intercept of the straight line with y-axis after extrapolation; it is thus the theoretical pressure increase in the absence of lipids ( $\pi_{\text{initial}} = 0$  mN/m).

Linear regression for N-L and DH-L resulted in Eqs. (1) and (2), respectively, with respective determination coefficients ( $R^2$ ) of 0.96 and 0.91.

$$y = -0.21x + 8.75 \quad (1)$$

$$y = -0.15x + 9.10 \quad (2)$$

The MIP is higher with DH-L than with N-L (59.6 and 41.5 mN/m, respectively; Table 1). The synergy factor as introduced by Boisselier et al. [24] and Calvez et al. [23] is also higher with DH-L than with N-L, and is positive for both proteins (0.85 and 0.79, respectively; Table 1) [24]. Oppositely, the  $\Delta\pi_0$  are similar for N-L and DH-L (8.75 and 9.10 mN/m, respectively; Table 1). It is noticeable that these latter values are smaller than the experimental surface pressure increase observed for N-L and DH-L lysozymes at the air/liquid interface at the same subphase concentration (10 and 11 mN/m, respectively).

The rate constant of adsorption  $k_{\text{ads}}$  ( $\text{M}^{-1} \text{s}^{-1}$ ) of a lysozyme solution with a concentration ( $c$ ) of 0.1  $\mu\text{M}$  at the air/liquid interface and the LPS/liquid interface can be evaluated by fitting the Langmuir Eq. (3) for adsorption to the surface pressure measurements. The rate constant of desorption  $k_{\text{des}}$  ( $\text{M}^{-1} \text{s}^{-1}$ ) can here be considered negligible.

$$\pi(t) = \pi_{\text{final}}(1 - \exp(-\sigma t)) \quad (3)$$

$$\sigma = k_{\text{ads}}c + k_{\text{des}} \quad (4)$$

At the air/liquid interface, N-L and DH-L have a  $k_{\text{ads}}$  value of  $6.6 \cdot 10^2 \text{ M}^{-1} \text{s}^{-1}$  and  $6.4 \cdot 10^2 \text{ M}^{-1} \text{s}^{-1}$ , respectively. The rate constants of adsorption for N-L and DH-L at the LPS/liquid interface of  $1.7 \cdot 10^3 \text{ M}^{-1} \text{s}^{-1}$  and  $1.3 \cdot 10^3 \text{ M}^{-1} \text{s}^{-1}$ , respectively, are higher than the rate constants of adsorption at the air/liquid interface. Thus, lysozyme adsorption at the air/liquid interface is slower than adsorption at the LPS/liquid interface. The differences in  $k_{\text{ads}}$  for N-L and DH-L for both the air/liquid and the LPS/liquid interface are not significant.

#### 3.3. Changes of surface pressure ( $\pi$ ) and ellipsometric angle ( $\Delta$ ) of LPS monolayer in the presence of lysozyme

Kinetics of the  $\pi$  and  $\Delta$  changes after injection of N-L and DH-L in the subphase was recorded using a LPS monolayer with an initial surface

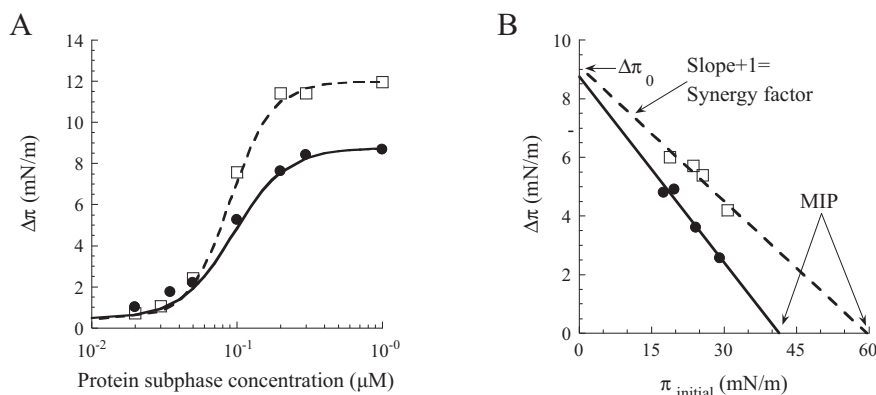


**Fig. 1.** A) Surface pressure increase ( $\Delta\pi$ ) of a LPS monolayer ( $\pi_{\text{initial}} = 18$  mN/m) induced by different subphase concentrations of native lysozyme (N-L) (●) and dry-heated lysozyme (DH-L) (□). B) Surface pressure increase of a LPS monolayer induced by 0.1  $\mu\text{M}$  N-L (●) and DH-L (□), depending on the initial surface pressure ( $\pi_{\text{initial}}$ ); the maximal insertion pressure (MIP) and the theoretical pressure increase in the absence of lipids ( $\Delta\pi_0$ ) are indicated by arrows.

**Table 1**

Binding parameters calculated for N-L and DH-L adsorption at a LPS monolayer: maximal insertion pressure (MIP), synergy factor, and theoretical pressure increase in the absence of lipids ( $\Delta\pi_0$ ); these parameters were extrapolated from the  $\Delta\pi$  vs.  $\pi_{\text{initial}}$  plots for 0.1  $\mu\text{M}$  lysozyme. For comparison, the surface pressure increase resulting from 0.1  $\mu\text{M}$  lysozyme adsorption at the air/liquid interface is indicated ( $\Delta\pi_{\text{final}}$ ).

		N-L	DH-L
LPS/liquid interface	MIP (mN/m)	41.5	59.6
	Synergy factor	0.79	0.85
	Theoretical $\Delta\pi_0$ (mN/m)	8.75	9.10
Air/liquid interface	$\Delta\pi_{\text{final}}$ (mN/m)	10	11

pressure of 25 mN/m and 30 mN/m, respectively. Different initial surface pressures of the LPS monolayers were chosen because of the different insertion capacities of N-L and DH-L for this experiment. The aim of this study is to evaluate the effects of N-L or DH-L on the LPS monolayer after a similar insertion of proteins, i.e. a similar  $\Delta\pi$ . The initial surface pressures which correspond to this prerequisite is 25 mN/m and 30 mN/m for a concentration of 0.1  $\mu\text{M}$  N-L and DH-L, respectively (Fig. 1B); more so, LPS monolayers with an initial surface pressure of 25 mN/m and 30 mN/m have similar  $\Delta$  values (supplementary data S1). The injection of N-L and DH-L under the LPS monolayer in these conditions results in a surface pressure increase of 2.9 mN/m and 3.5 mN/m, respectively (Fig. 2A), and induces an increase of ellipsometric angle of 8° and 12°, respectively (Fig. 2B).

#### 3.4. Changes of surface pressure ( $\pi$ ) and ellipsometric angle ( $\Delta$ ) of KLA monolayer in the presence of lysozyme

To estimate the influence of the polysaccharide moieties on lysozyme interactions with LPS monolayer, KLA lipids were used. KLA lipids are derivative forms of LPS from which the polysaccharide moiety besides two 3-deoxy-D-manno-octulosonic acid (KdO) groups are missing (Fig. 3). The use of KLA was also relevant to test the role of electrostatic interactions between lysozyme and the negative charge at the interface by making the access to the charge easier. KLA monolayers are homogeneous lipid films on the contrary to LPS monolayers. This was confirmed by AFM imaging (supplementary data S2).

Kinetics of the  $\pi$  and  $\Delta$  changes after injection of N-L and DH-L in the subphase was recorded for a KLA monolayer with an initial surface pressure of 25 mN/m and 30 mN/m, respectively. For N-L, the surface pressure of the KLA monolayer is stable for the first half hour and then decreases after 3 h (−2.1 mN/m) (Fig. 4A). Oppositely, DH-L injection induces an immediate and more intense decrease (−5 mN/m after 3 h) (Fig. 4A). Both N-L and DH-L interact with the

KLA monolayer in such a way that the ellipsometric angle increases slightly after injection of both proteins: +0.65° and +1.5° after 3 h, respectively (Fig. 4B).

#### 3.5. Microscopic observations of LPS monolayer in the presence of lysozyme

Brewster angle microscopy (BAM) and ellipsometry were performed to visualize the LPS monolayer organization on a  $\mu\text{m}$ -scale before and after lysozyme injection in the subphase. BAM-images give information on the thickness and refraction index of the LPS monolayer. Thick and/or high refraction index zones will appear lighter (white) than thin and low index zones (black). Delta maps show the same information as the BAM images, but the differences in height and/or refraction index are more precisely measured. Blue is the baseline color of the delta maps and correspond to a small delta value. High delta zones will be represented from green till red.

Before lysozyme injection, the LPS monolayer is heterogeneous, with black and white zones, at both initial surface pressures (25 mN/m and 30 mN/m), as evidenced by BAM-imaging (Fig. 5A and E). In the absence of literature references, the black colored zones are assumed to correspond to LPS with short polysaccharide chains (low refractive index and low thickness), while the white regions are assumed to correspond to LPS with long polysaccharide chains (high refractive index and high thickness). Such domain-organization is likely considering the optimal thermodynamic configuration that suggests segregation of LPS with similar polysaccharide chain lengths. The same information is provided by the delta-maps (Fig. 5C and G).

One hour after injection of 0.1  $\mu\text{M}$  N-L, the BAM-images and delta-maps do not show any significant change of the heterogeneity as compared to the initial LPS monolayer (Fig. 5B and D), despite a slight increase of the background  $\Delta$ -value in the delta-map (Fig. 5D). On the contrary, after injection of DH-L, an unequivocal change of the LPS monolayer organization is observed in both BAM-images and delta-maps (Fig. 5F and H). Especially, the small high  $\Delta$ -domains make place for bigger ones, and the background  $\Delta$ -value increases (Fig. 5H).

Atomic force microscopy (AFM) enables to investigate the LPS monolayer at a nanoscale with a high resolution. Thus, this technique was used to study more precisely the organization of the lipid monolayer observed in the background of BAM-images (black zones).

The resulting AFM-images show the heterogeneity of the initial LPS monolayer at a nanoscale at both initial surface pressures (25 mN/m and 30 mN/m; Fig. 6A, C, E and G). The height difference between the lower (zone 1) and higher (zone 2) lipid zones is 1.2 to  $2.0 \pm 0.2$  nm. By grating the LPS (data not shown), the monolayer thickness could be measured and corresponds to 5 nm. The monolayer thickness is in coherence with the one found by Le Brun et al. [26].

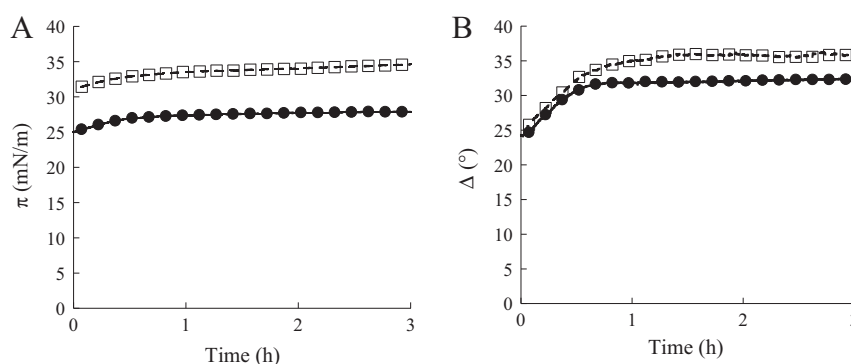


**Fig. 2.** Surface pressure  $\pi$  (A) and ellipsometric angle  $\Delta$  (B) changes during N-L (●) and DH-L (□) adsorption at a LPS monolayer having an initial surface pressure of 25 mN/m and 30 mN/m, respectively.

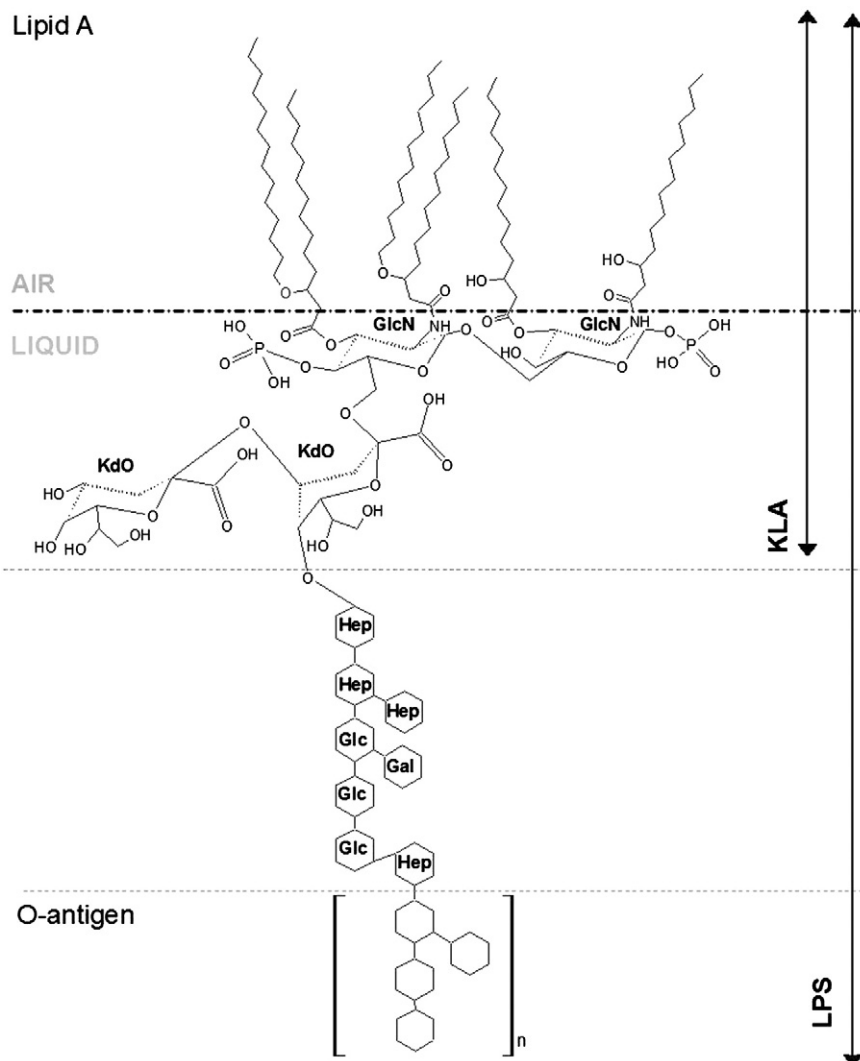


**Fig. 3.** Schematic representation of *E. coli* K12 LPS and KLA lipids. GlcN (*N*-acetylglucosamine); KdO (3-deoxy-D-manno-octulosonic acid); Hep (*L*-glycero-D-manno heptose); Gal (galactose); Glc (glucose).

The impact of N-L and DH-L on the lipid monolayer can also be studied by AFM, enabling to study more carefully the reorganization of the low  $\Delta$ -domains present in the BAM-images.

AFM shows that the injection of 0.1  $\mu$ M N-L or DH-L does not significantly modify the heterogeneous appearance of the LPS monolayer

(Fig. 6B, D, F and H). However, the insertion and adsorption of 0.1  $\mu$ M N-L gives rise to the formation of small domains (object 1) with a height of  $1.4 \pm 0.4$  nm (Fig. 6B and D). The height of these domains is equivalent to the height of the dense domains observed in absence of lysozyme (Fig. 6A and C). The adsorption and insertion of 0.1  $\mu$ M

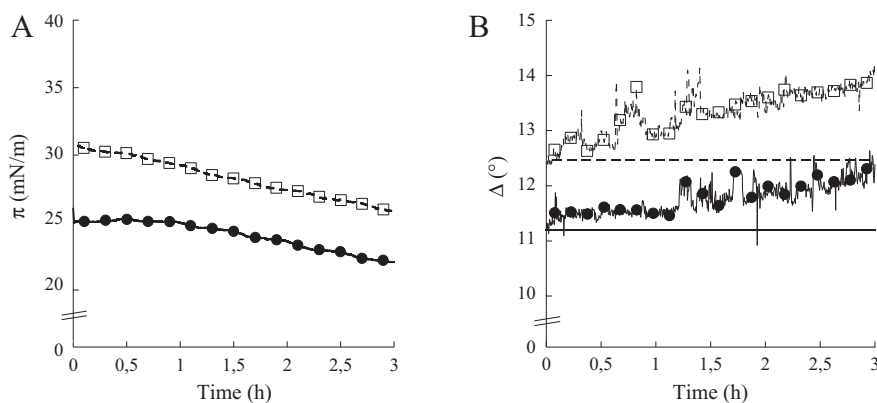


**Fig. 4.** Surface pressure  $\pi$  (A) and ellipsometric angle  $\Delta$  (B) changes during N-L (●) and DH-L (□) adsorption at a KLA monolayer having an initial surface pressure of 25 mN/m and 30 mN/m, respectively. The initial  $\Delta$ s of the KLA lipids at 25 mN/m and 30 mN/m are shown as full and dashed lines, respectively.



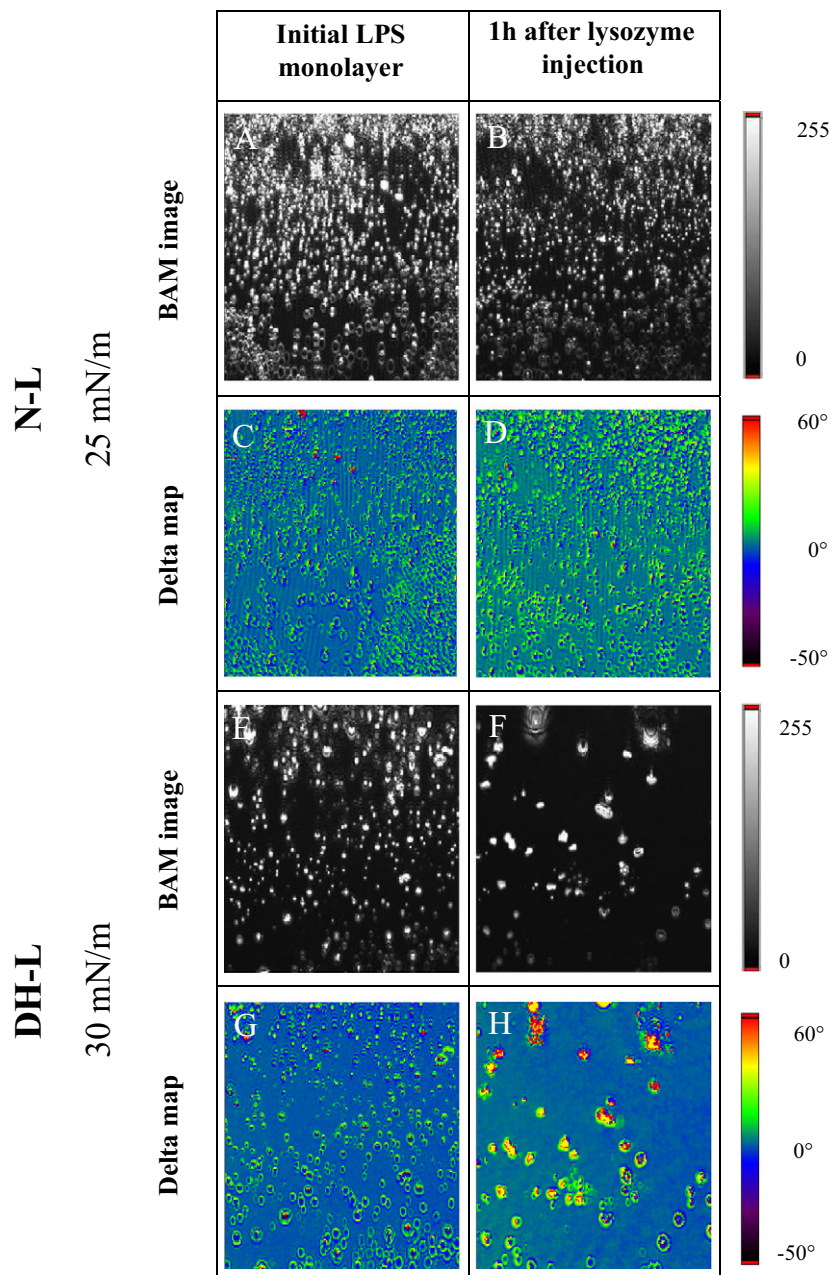


**Fig. 5.** BAM-images and delta-maps ( $450\ \mu\text{m} \times 390\ \mu\text{m}$ ) before (A, C, E, G) and after N-L (B, D) or DH-L (F, H) injection under the LPS monolayer. The initial surface pressure was 25 mN/m or 30 mN/m, for N-L or DH-L, respectively.

DH-L induces the formation of two types of clusters (objects 2 and 3 with a height of  $25 \pm 5$  and  $57 \pm 12$  nm, respectively) and small domains (object 4) ( $1.4 \pm 0.3$  nm height) (Fig. 6F and H).

Topographical information shown in the AFM images is representative for the whole sample. However, the size and shape of the different domains is irregular and heterogeneously distributed over the sample, making it impossible to quantify the effect of lysozyme on the domain size and shape.

#### 4. Discussion

Native lysozyme (N-L) has been shown active against Gram-negative bacteria such as *E. coli* [11,27]. Membrane permeabilization has been suggested as one of the mechanisms responsible for this activity [8,28]. This assumption was recently confirmed by our group who demonstrated

that N-L causes the formation of pores and ion channels in the outer and cytoplasmic membranes, respectively [9,11]. Pore formation due to N-L implies that interactions occur between the protein and the *E. coli* outer membrane. Nevertheless, the mode of insertion of lysozyme into the outer membrane remains unknown.

Moreover, dry-heated lysozyme (DH-L) has a higher antimicrobial activity and higher membrane disruption potential than N-L [11]. This improved activity is supposed to be related to the modified physico-chemical properties of DH-L. DH-L is more hydrophobic, flexible and surface active than N-L, but its secondary and tertiary structures remain intact [29,30]. It is thus relevant to compare the interaction of native and dry-heated lysozymes with LPS, the lipid components of the outer leaflet of the outer membrane of Gram negative bacteria.

Interfacial monolayers are considered as good models to study interactions between antimicrobial peptides and bacterial membranes [18,

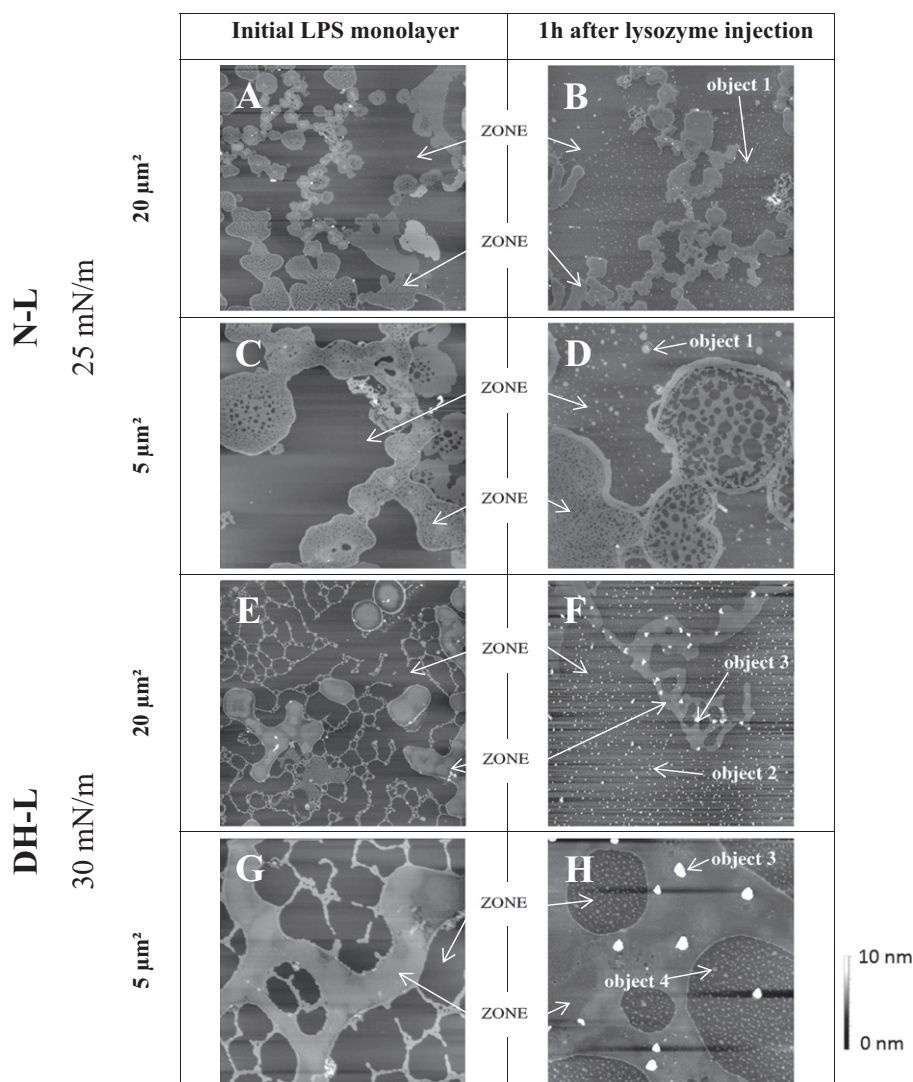


**Fig. 6.** Topographic AFM-images before (A, C, E, G) and after N-L (B, D) or DH-L (F, H) injection under the LPS-monolayer. The initial surface pressure was 25 mN/m or 30 mN/m, for N-L or DH-L, respectively. The Z-range is 10 nm.

19]. In the presently reported study, a LPS monolayer was used to mimic the outer leaflet of the *E. coli* K12 outer membrane, in order to explore the first step of lysozyme interaction with bacterial membrane. It is noticeable that wild-type LPS was here used for the first time to investigate protein-LPS interactions at a macroscopic and mesoscopic level, using biophysical tools such as tensiometry, ellipsometry, AFM and BAM.

#### 4.1. The affinity of N-L for LPS is very high and makes possible the insertion of the protein into a LPS monolayer

For the first time, protein insertion into a wild type LPS monolayer is here demonstrated. Until now, protein insertion was only recorded for LPS-derivative monolayers and lung surfactant protein D. [31]. The

**Table 2**  
Surface pressure increase ( $\Delta\pi$ ) of LPS or LPS-derivative monolayers measured after adsorption of antimicrobial peptides and N-L or DH-L. The initial surface pressure was 18 mN/m for both peptides and protein.

	Peptide or protein	Concentration ( $\mu\text{M}$ )	$\Delta\pi$ (mN/m)	Bacterial species	LPS type	Reference
Peptides	Polymyxin B (1.4 kDa)	0.5	17.5	<i>S. enterica</i>	Re-LPS	[32]
	Polymyxin E1 (1.2 kDa)	0.5	21	<i>S. enterica</i>	Re-LPS	[32]
	Colymycin (1.8 kDa)	0.5	0.5	<i>S. enterica</i>	Re-LPS	[32]
	Gramicidin S (1.1 kDa)	0.15	17	<i>S. enterica</i>	Re-LPS	[32]
	Temporin L (1.6 kDa)	0.1	7.5	<i>E. coli</i>	Wild-type LPS	[33]
Lysozyme	N-L (14.4 kDa)	0.1	5.2	<i>E. coli</i>	Wild-type LPS	This study
	N-L (14.4 kDa)	0.1	−2.1	<i>E. coli</i>	KLA ~ Re-LPS	This study
	DH-L (14.4 kDa)	0.1	7.8	<i>E. coli</i>	Wild-type LPS	This study
	DH-L (14.4 kDa)	0.1	−5	<i>E. coli</i>	KLA ~ Re-LPS	This study

surface pressure increase measured when N-L is injected into the sub-phase demonstrates that N-L is able to insert into a LPS monolayer (Fig. 1A). The ability of lysozyme to interact with LPS is consistent with the surface activity of the protein at the air/liquid interface [30]. However, insertion of N-L into the LPS monolayer remains lower than for antimicrobial peptides such as temporin L, as suggested by the lower surface pressure increase (Table 2) [32,33]. The larger molecular size and higher rigidity of lysozyme [34], as compared to peptides, could be responsible for the lower efficiency of the protein.

The maximal insertion pressure (MIP), determined from measurements of N-L insertion at different initial pressures, is high (41.5 mN/m, Table 1) and similar to MIP recorded for antimicrobial peptides and phospholipid monolayers (25–45 mN/m) [23,33]. Especially, it is remarkable that the MIP value is higher than the lateral pressure which is supposed to exist in natural membrane systems in eukaryotic cells (~30 mN/m) [35]. Unfortunately, no measurements or theoretical deductions of the lateral pressure in the outer and cytoplasmic membranes of prokaryotes are available in literature then no comparison is possible with the here observed MIP value. Moreover, the N-L synergy factor (0.79, Table 1) is extremely high as compared to reported values for protein insertion into phospholipid monolayers (from 0.3 to 0.5) [24]. It can thus be concluded that the protein has a high affinity for the LPS interface between 18 and 30 mN/m and strikingly lysozyme insertion is almost not impacted by the lateral cohesion of the LPS molecules. These observations suggest a mode of action that is unusual compared to the interaction between protein and phospholipids. This could result from the LPS inherent molecular structure and from the specificities of a LPS monolayer compared to a phospholipid monolayer; the LPS molecules have heterogeneous polysaccharide chains in length, thus the monolayer has a variable thickness induced by the auto-assembly of similar LPS molecules observed by BAM and AFM microscopy (Figs. 5 and 6). Indeed, a LPS monolayer can be divided into two distinct zones, i.e. a polysaccharide zone and a phospholipid-like zone, on the contrary to a phospholipid monolayer which is composed of a unique zone.

#### 4.2. The polysaccharide moieties of LPS are needed for N-L insertion

When LPS molecules are depleted from their polysaccharide moieties (KLA), lysozyme is no longer able to insert into the lipid monolayer, since no increase of the surface pressure occurs (Fig. 4A). However, lysozyme adsorption is evidenced by the increase of the ellipsometric angle ( $\Delta$ ) (Fig. 4B). Lysozyme adsorption could involve hydrogen bonds between the protein and the remaining two sugar moieties, or electrostatic interactions between the positive lysozyme and the negative KLA. The latter assumption is reinforced by the immediate and higher adsorption of DH-L which is more positively charged than N-L (Fig. 2B). It is also in accordance with Brandenburg et al. who reported electrostatic interactions between *Salmonella minnesota* Re-LPS and lysozyme in solution [36].

Actually, while N-L adsorption is proceeding for 3 h (Fig. 4B), the surface pressure of the lipid monolayer is decreasing (Fig. 4A). This could be due to a destabilization and partial solubilization of the lipid monolayer as has been previously described for the antimicrobial peptide protegrin-1 at a lipid A monolayer [37]; another hypothesis is the reorganization or reorientation of the lipid headgroups induced by lysozyme presence beneath the monolayer, similar to what has been previously reported for a dystrophin subdomain R20–24 at a DOPC/DOPS monolayer [38]. If a partial solubilization of the KLA occurs, this should be reflected in a decrease of the ellipsometric angle ( $\Delta$ ), due to the loss of matter at the interface. Here, the ellipsometric angle increases (Fig. 4), meaning that rather than a solubilization of the KLA monolayer, a reorganization of the KLA head groups takes place leading to a relaxation of the lipid film. Lysozyme molecules are trapped beneath the KLA monolayer caused by strong electrostatic attractive forces between lysozyme and the KLA lipids.

On the contrary, when N-L interacts with a LPS monolayer, i.e. including polysaccharide moieties, surface pressure and ellipsometric angle simultaneously increase (Fig. 2A and B). Undoubtedly, N-L is thus able to insert deeply in the interface, up to the hydrophobic zone of the LPS monolayer. A hypothesis can be the effect of steric hindrance of the polysaccharides which prevents total coverage of the interface by the lipid headgroups, thus leaving free space for lysozyme insertion. Moreover, the polysaccharide chains can also cause simultaneously partial shielding of the negative charges on the headgroups and therefore prevent the entrapment of the positive lysozyme molecules at the level of these negative charges as it is the case for KLA lipids. The decreased interaction of the negative charges with positive lysozyme could enable insertion of the protein between the LPS headgroups. At last, lysozyme and the polysaccharides moieties could interact and create compact zones as LPS/lysozyme domains and complexes (Fig. 6) resulting in lesser density in other areas enabling the remaining free lysozyme to attain the interface. Such strong hydrophobic interactions have already been reported between LPS and lysozyme in solution [39], and LPS/lysozyme complexes have been observed [36,40].

#### 4.3. N-L interaction with LPS causes a slight reorganization of the LPS monolayer

At the same time as the surface pressure increases when N-L is injected under a LPS monolayer, a strong increase of the ellipsometric angle  $\Delta$  (+7°, Fig. 2B) is observed, which is higher than the ellipsometric angle increase for protein/phospholipid monolayers [41]. This unusually high  $\Delta$  increase can be explained by the LPS/lysozyme complex formation, polysaccharide reorganization, and/or the presence of N-L at the interface, since the ellipsometric angle depends on the refraction index and the film thickness.

BAM and AFM imaging were performed to evaluate the different hypotheses explaining the  $\Delta$  increase. BAM and AFM imaging show the heterogeneity of the initial LPS monolayer at micrometer and nanometer scales, respectively (Figs. 4A, C and 5A, C), as a result of the variable lengths of the polysaccharides chains. After N-L injection and interaction with LPS, this heterogeneity is maintained as can be observed in the BAM (Fig. 5B and D) and AFM images (Fig. 6B and D). But N-L injection also results in a slight increase of the background  $\Delta$ -value in the delta-map (Fig. 5D), and in the formation of small domains on the background zones in AFM-imaging (Fig. 6B and D). It can thus be concluded that N-L reorganizes the LPS monolayer, even if this reorganization remains limited. The reorganization of the LPS monolayer and the LPS/lysozyme complex formation could possibly be the preliminary steps for pore formation by N-L as observed *in vivo* by Derde et al. [9].

#### 4.4. DH-L has a stronger affinity for LPS than N-L, and causes more radical reorganization of the LPS monolayer

Similarly to N-L, DH-L insertion into the LPS monolayer is enabled by the polysaccharides moieties, and DH-L reorganizes the LPS monolayer. However, differences in the behavior of DH-L versus N-L with the LPS monolayer can be noticed. This modified behavior could be related to its different physico-chemical properties such as increased hydrophobicity, surface-activity, positive charge and flexibility [29,30].

DH-L insertion into the LPS monolayer is more efficient than N-L at concentrations higher than 0.05  $\mu$ M (Fig. 1A). This could be due to the higher flexibility of DH-L as compared to N-L [29], which could allow more DH-L molecules to insert into the LPS monolayer, and/or to restructure more efficiently the interface. The increased insertion capacity of DH-L is consistent with its slight increased interfacial behavior ( $\pi_{\text{final}}$ , Table 1). Especially, it is noticeable that the surface pressure increase induced by DH-L insertion into the LPS-monolayer is similar to that measured with an antimicrobial peptide, i.e. temporin L, in equivalent



conditions (Table 2). DH-L has also more affinity for the LPS monolayer than N-L, demonstrated by its higher MIP and synergy factor (59.6 mN/m and 0.85, respectively; Table 1) [23,33]. The drastically different reorganization of the LPS monolayer by DH-L is highlighted by BAM and AFM imaging (Figs. 5 and 6). The BAM-images show that the many small domains with a high  $\Delta$ -value visible in the presence of N-L (Fig. 5B and D) are replaced by larger and fewer high  $\Delta$ -value domains in the presence of DH-L (Fig. 5F and H). Concurrently, more or less thick, and more or less large clusters appear in the presence of DH-L, as evidenced by AFM images (Fig. 6F and H). These clusters could be protein aggregates caused by high local concentration of DH-L at the LPS-monolayer, consistently with the higher sensitivity to aggregation of DH-L as compared to N-L, previously established by Desfougères et al. [30].

## 5. Conclusions

The presently reported study demonstrates the strong interaction between N-L and a LPS monolayer, usually considered as a relevant model of the outer membrane of Gram-negative bacteria. Even more, N-L is able to insert leading to a lateral reorganization of the LPS monolayer, which can explain pore formation into the *E. coli* outer membrane, previously observed *in vivo* [11]. An original and unexpected result is that lysozyme insertion between the lipid A of LPS monolayers requires the presence of the polysaccharide moieties. This reveals specific interactions between lysozyme and the polysaccharide moieties leading to better insertion and decreased electrostatic attraction. Further experiments are needed in order to settle between the different hypotheses that could explain this finding.

Moreover, dry-heating modifies lysozyme properties in such a way that its affinity for LPS, its insertion capacity, and its ability for LPS monolayer reorganization are emphasized. These results are thus consistent with *in vivo* experiments that demonstrated larger and/or more numerous pores induced by DH-L into the *E. coli* outer membrane, as compared to N-L [11].

The interaction of N-L and DH-L with the outer membrane lipids is now well established and consistent with the pore formation previously demonstrated *in vivo*. Self-uptake mechanism is then imaginable meaning that lysozyme molecules involved in pore formation and stabilization could enable the entrance of free lysozyme in the bacterial cell. Then, it is relevant to further study the interaction of lysozyme with the cytoplasmic membrane, the final hurdle before access to the cytoplasm. The findings resulting from this study are currently analyzed and will soon be published.

## Acknowledgment

The authors thank “Conseil Régional de Bretagne” for the funding of this work.

## Appendix A. Supplementary data

Additional experimental data on the ellipsometric angle of a LPS monolayer (S1), atomic force images of LPS or KLA monolayers (S2) and isothermal compression of LPS and KLA monolayers (S3). This material is available free of charge via the Internet at <http://pubs.acs.org>. Supplementary data related to this article can be found online at DOI: <http://dx.doi.org/10.1016/j.bbame.2014.10.026>.

## References

- [1] World Health Organization, Overcoming antimicrobial resistance, Geneva, Switzerland, 2000.
- [2] A. Rosbach, Report on the microbial challenge—Rising threats from antimicrobial resistance (2012/2041 (INI)), European parliament, committee on the environment, public health and food safety, 2012.
- [3] L.T. Nguyen, E.F. Haney, H.J. Vogel, The expanding scope of antimicrobial peptide structures and their modes of action, *Trends Biotechnol.* 29 (2011) 464–472.
- [4] A. Peschel, H.G. Sahl, The co-evolution of host cationic antimicrobial peptides and microbial resistance, *Nat. Rev. Microbiol.* 4 (2006) 529–536.
- [5] H. Jenssen, P. Hamill, R.E. Hancock, Peptide antimicrobial agents, *Clin. Microbiol. Rev.* 19 (2006) 491–511.
- [6] P. Jolles, J. Jolles, What's new in lysozyme research—always a model system, today as yesterday, *Mol. Cell. Biochem.* 63 (1984) 165–189.
- [7] B. Masschalck, C.W. Michiels, Antimicrobial properties of lysozyme in relation to foodborne vegetative bacteria, *Crit. Rev. Microbiol.* 29 (2003) 191–214.
- [8] A. Pellegrini, U. Thomas, P. Wild, E. Schraner, R. von Fellenberg, Effect of lysozyme or modified lysozyme fragments on DNA and RNA synthesis and membrane permeability of *Escherichia coli*, *Microbiol. Res.* 155 (2000) 69–77.
- [9] M. Derde, V. Lechevalier, C. Guérin-Dubiard, M.F. Cochet, S. Jan, F. Baron, et al., Hen egg white lysozyme permeabilizes the *Escherichia coli* outer and inner membranes, *J. Agric. Food Chem.* 61 (2013) 9922–9929.
- [10] K. Düring, P. Porsch, A. Mahn, O. Brinkmann, W. Gieffers, The non-enzymatic microbicidal activity of lysozymes, *FEBS Lett.* 449 (1999) 93–100.
- [11] M. Derde, C. Guérin-Dubiard, V. Lechevalier, M.-F. Cochet, S. Jan, F. Baron, et al., Dry-heating of lysozyme increases its activity against *Escherichia coli* membranes, *J. Agric. Food Chem.* 62 (2014) 1692–1700.
- [12] Y. Mine, F.P. Ma, S. Lauriau, Antimicrobial peptides released by enzymatic hydrolysis of hen egg white lysozyme, *J. Agric. Food Chem.* 52 (2004) 1088–1094.
- [13] A.M. Abdou, S. Higashiguchi, A. Abouleinin, M. Kim, H.R. Ibrahim, Antimicrobial peptides derived from hen egg lysozyme with inhibitory effect against *Bacillus* species, *Food Control* 18 (2007) 173–178.
- [14] H.R. Ibrahim, S. Higashiguchi, L.R. Juneja, M. Kim, T. Yamamoto, A structural phase of heat-denatured lysozyme with novel antimicrobial action, *J. Agric. Food Chem.* 44 (1996) 1416–1423.
- [15] M. Hoq, I.K. Mitsuno, Y. Tsujino, T. Aoki, H.R. Ibrahim, Triclosan-lysozyme complex as novel antimicrobial macromolecule: a new potential of lysozyme as phenolic drug-targeting molecule, *Int. J. Biol. Macromol.* 42 (2008) 468–477.
- [16] H.R. Ibrahim, A. Kato, K. Kobayashi, Antimicrobial effects of lysozyme against Gram-negative bacteria due to covalent binding of palmitic acid, *J. Agric. Food Chem.* 39 (1991) 2077–2082.
- [17] H.R. Ibrahim, M. Yamada, K. Kobayashi, A. Kato, Bactericidal action of lysozyme against Gram-negative bacteria due to insertion of a hydrophobic pentapeptide into its C-terminus, *Biosci. Biotechnol. Biochem.* 56 (1992) 1361–1363.
- [18] H. Brockman, Lipid monolayers: why use half a membrane to characterize protein-membrane interactions? *Curr. Opin. Struct. Biol.* 9 (1999) 438–443.
- [19] S. Roes, U. Seydel, T. Gutschmann, Probing the properties of lipopolysaccharide monolayers and their interaction with the antimicrobial peptide polymyxin B by atomic force microscopy, *Langmuir* 21 (2005) 6970–6978.
- [20] ExPASy, P00698 (Chicken lysozyme), (n.d.). <http://web.expasy.org/cgi-bin/protparam/protparam1?P00698@19-147@> (accessed April 2, 2014).
- [21] B. Berge, A. Renault, Ellipsometry study of 2D crystallization of 1-alcohol monolayers at the water surface, *EPL Europhys. Lett.* 21 (1993) 773.
- [22] R.M.A. Azzam, N.M. Bashara, Ellipsometry and polarized light, North-Holland Pub. Co., 1977.
- [23] P. Calvez, S. Bussièrès, Éric Demers, C. Sables, Parameters modulating the maximum insertion pressure of proteins and peptides in lipid monolayers, *Biochimie* 91 (2009) 718–733.
- [24] É. Boisselier, P. Calvez, É. Demers, L. Cantin, C. Sables, Influence of the physical state of phospholipid monolayers on protein binding, *Langmuir* 28 (2012) 9680–9688.
- [25] P. Calvez, E. Demers, E. Boisselier, C. Sables, Analysis of the contribution of saturated and polyunsaturated phospholipid monolayers to the binding of proteins, *Langmuir* 27 (2011) 1373–1379.
- [26] A.P. Le Brun, L.A. Clifton, C.E. Halbert, B. Lin, M. Meron, P.J. Holden, et al., Structural characterization of a model Gram-negative bacterial surface using lipopolysaccharides from rough strains of *Escherichia coli*, *Biomacromolecules* 14 (2013) 2014–2022.
- [27] A. Pellegrini, U. Thomas, R. Vonfellenberg, P. Wild, Bactericidal activities of lysozyme and aprotinin against Gram-negative and Gram-positive bacteria related to their basic character, *J. Appl. Bacteriol.* 72 (1992) 180–187.
- [28] P. Wild, A. Gabrieli, E.M. Schraner, A. Pellegrini, U. Thomas, P.M. Frederik, et al., Reevaluation of the effect of lysozyme on *Escherichia coli* employing ultrarapid freezing followed by cryoelectron microscopy or freeze substitution, *Microsc. Res. Tech.* 39 (1997) 297–304.
- [29] Y. Desfougères, J. Jardin, V. Lechevalier, S. Pézenne, F. Nau, Succinimidyl residue formation in hen egg-white lysozyme favors the formation of intermolecular covalent bonds without affecting its tertiary structure, *Biomacromolecules* 12 (2011) 156–166.
- [30] Y. Desfougères, A. Saint-Jalmes, A. Salonen, V. Vié, S. Beaufils, S. Pézenne, et al., Strong improvement of interfacial properties can result from slight structural modifications of proteins: the case of native and dry-heated lysozyme, *Langmuir* 27 (2011) 14947–14957.
- [31] L. Wang, J.W. Brauner, G. Mao, E. Crouch, B. Seaton, J. Head, et al., Interaction of recombinant surfactant protein D with lipopolysaccharide: conformation and orientation of bound protein by IRRAS and simulations, *Biochemistry* 47 (2008) 8103–8113.
- [32] L. Zhang, P. Dhillon, H. Yan, S. Farmer, R.E.W. Hancock, Interactions of bacterial cationic peptide antibiotics with outer and cytoplasmic membranes of *Pseudomonas aeruginosa*, *Antimicrob. Agents Chemother.* 44 (2000) 3317–3321.
- [33] A. Giacometti, O. Cirioni, R. Ghiselli, F. Mocchegiani, F. Orlando, C. Silvestri, et al., Interaction of antimicrobial peptide temporin L with lipopolysaccharide *in vitro* and in experimental rat models of septic shock caused by Gram-negative bacteria, *Antimicrob. Agents Chemother.* 50 (2006) 2478–2486.
- [34] R.E. Canfield, A.K. Liu, The disulfide bonds of egg white lysozyme (muramidase), *J. Biol. Chem.* 240 (1965) 1997–2002.
- [35] D. Marsh, Lateral pressure in membranes, *Biochim. Biophys. Acta* 1286 (1996).

- [36] K. Brandenburg, M.H. Koch, U. Seydel, Biophysical characterisation of lysozyme binding to LPS Re and lipid A, *Eur. J. Biochem.* 258 (1998) 686–695.
- [37] Y. Ishitsuka, D. Pham, A. Waring, R. Lehrer, K. Lee, Insertion selectivity of antimicrobial peptide protegrin-1 into lipid monolayers: effect of head group electrostatics and tail group packing, *Biochim. Biophys. Acta BBA-Biomembr.* 1758 (2006) 1450–1460.
- [38] V. Vié, S. Legardinier, L. Chieze, O. Le Bihan, Y. Qin, J. Sarkis, et al., Specific anchoring modes of two distinct dystrophin rod sub-domains interacting in phospholipid Langmuir films studied by atomic force microscopy and PM-IRRAS, *Biochim. Biophys. Acta BBA-Biomembr.* 1798 (2010) 1503–1511.
- [39] N. Ohno, D.C. Morrison, Lipopolysaccharide interaction with lysozyme. Binding of lipopolysaccharide to lysozyme and inhibition of lysozyme enzymatic activity, *J. Biol. Chem.* 264 (1989) 4434–4441.
- [40] N. Ohno, N. Tanida, T. Yadomae, Characterization of complex-formation between lipopolysaccharide and lysozyme, *Carbohydr. Res.* 214 (1991) 115–130.
- [41] J. Sarkis, J.-F. Hubert, B. Legrand, E. Robert, A. Chéron, J. Jardin, et al., Spectrin-like repeats 11–15 of human dystrophin show adaptations to a lipidic environment, *J. Biol. Chem.* 286 (2011) 30481–30491.